Investigation on Dynamics of the Extended Duffing-Van der Pol System

Jun Yu[a] and Jieru Li[b]

[a] Institute of Nonlinear Science, Shaoxing University, Shaoxing 312000, China
[b] School of Life Sciences, Sun Yat-sen University, Guangzhou 510275, China

Reprint requests to J. Y.; E-mail: junyu@zscas.edu.cn

Z. Naturforsch. **64a,** 341 – 346 (2009); received September 8, 2008 / revised October 18, 2008

The chaotic motion in periodic self-excited oscillators has been extensively investigated through experiments and computer simulations. However, with the advent of the study of chaotic motion by means of strange attractors, Poincaré map, fractal dimension, it has become necessary to seek for a better understanding of nonlinear system with higher order nonlinear terms. In this paper we consider an extended Duffing-Van der Pol oscillator by introducing a nonlinear quintic term. The dynamical behaviour of the system is investigated by using Melnikov analysis and numerical simulation. The results can help one to understand the essence of given nonlinear system.

Key words: Extended Duffing-Van der Pol Oscillator; Bifurcation; Chaos.

1. Introduction

In recent years the study of chaotic phenomena in the area of nonlinear periodic self-excited oscillators has attracted much attention [1 – 3]. Among the periodically forced self-excited oscillators, the most extensively studied example is the Duffing-Van der Pol oscillator, governed by the equation

$$\ddot{x} - \mu(1-x^2)\dot{x} + \omega_0^2 x + \beta x^3 = f(t), \tag{1}$$

where $\mu > 0$, ω_0 and β are constant parameters, and f is a function of time. Originally, it was a model for an electrical circuit with a triode. In fact, it serves as a basic model for self-excited oscillations in physics, engineering, electronics, biology, neurology and many other disciplines [4, 5]. It is therefore one of the most intensively studied systems in nonlinear dynamics [6]. The chaotic motion in this system was first explored and reported by Ueda and Akamatsu [7]. Since then many researchers were attracted to this topic and made contributions to the study of the mechanism of complex phenomenon observed from experiments and computer simulations. For instance, the authors of [8] showed that a Van der Pol oscillator with a double well potential possesses a rich dynamical behaviour with a vast number of states, the chaotic sea containing many islands of periodic and phase-locked states, and the transitions from chaos to regular states being through various routes: period-doubling phenomena, intermittencies, crises, transient chaos, and quasi-periodicity. Moukam Kakmeni et al. [6] studied the strange attractors and chaotic behaviour of an anharmonic DVP oscillator with two external forces by applying numerical calculations.

With the advent of the study of chaotic motion by means of strange attractors, Poincaré map, fractal dimension, it has become necessary to seek for a better understanding of nonlinear system with higher order nonlinear terms. In this paper we consider an extended Duffing-Van der Pol oscillator or ϕ^6-Van der Pol oscillator

$$\ddot{x} - \mu(1-x^2)\dot{x} + \alpha x + \beta x^3 + \delta x^5 = f(t), \tag{2}$$

where $\alpha = \omega_0^2$, δ is a constant parameter, and $f(t) = f\cos\omega t$ is an external excitation. The potential of which is the ϕ^6 potential given by

$$V(x) = \frac{\alpha}{2}x^2 + \frac{\beta}{4}x^4 + \frac{\delta}{6}x^6. \tag{3}$$

Depending on the set of the parameters, it can be considered at least three physically interesting situations where the potential is (i) single well, (ii) double well, and (iii) triple well. Each one of the above three cases has become a central model to describe inherently nonlinear phenomena, exhibiting a rich and baffling variety of regular and chaotic motions [8]. Figure 1 shows two forms of the potential $V(x)$ for $\alpha > 0$. Throughout this note we are only concerned with $\alpha > 0$ cases: a single well and triple well.

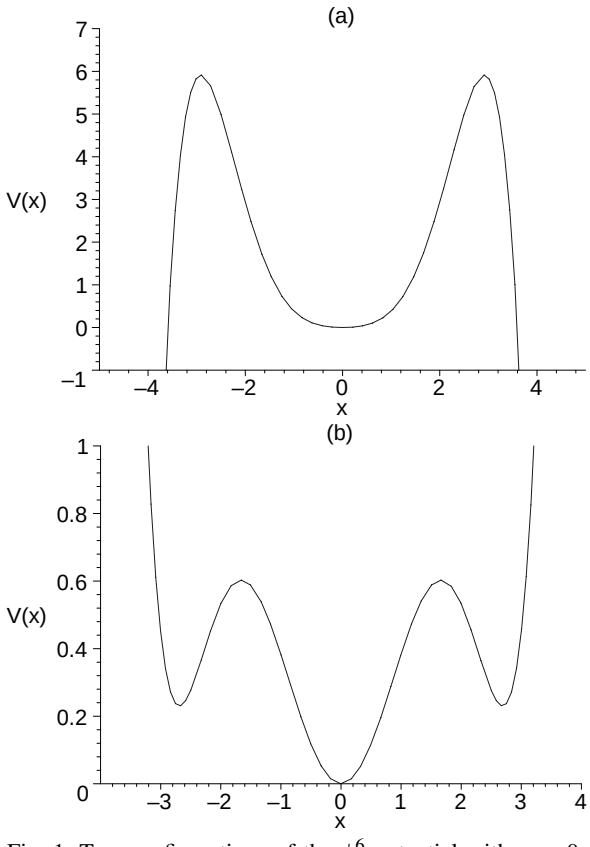

Fig. 1. Two configurations of the ϕ^6 potential with $\alpha > 0$: (a) single well for $\alpha = 0.4$, $\beta = 0.8$ and $\delta = -0.1$; (b) triple well for $\alpha = 1.0$, $\beta = -0.5$ and $\delta = 0.05$.

This ϕ^6-potential system has attracted much attention [9–11], due to the fact that it is a universal nonlinear differential equation, and many nonlinear oscillators in physical, engineering and biological problems can be really described by the model or analogous ones. For example, (2) has been utilized to model bistability in the multiple-photon absorption process, soft and hard springs, four-wave interaction and plasma oscillation [8]. The resonance and nonresonance oscillations of (2) was analyzed by using the multiple scale method and the condition for existence of homoclinic bifurcation was obtained by means of the Melnikov theory [9]. The effect of bounded noise on the chaotic motion of system (2) in a triple well potential was investigated through Poincaré maps [10]. In [11], the periodic and chaotic motions of (2) in the case of the single well potential have been observed with the aid of phase diagrams, and a novel robust control scheme using sliding mode approach was also proposed.

Nevertheless, the dynamical characteristic of chaotic motion and the routes to chaos taking place in this new system have not been described detailed. Especially, the understanding of the dynamical behaviour in the system is far from complete. Though a survey of chaotic behaviour of (2) has been made by employing phase diagrams in [11], it is very limited to understand a global picture of the system response. Thus a further investigation on this nonlinear system by numerical simulations including bifurcation diagram, phase projections and Poincaré map, as well as the spectrum of Lyapunov exponent and fractal dimension is needed.

In this work we will undertake an investigation of the dynamical behaviour of system (2) with a single well potential and triple well potential in some detail by using the Melnikov analysis and numerical simulation.

2. Melnikov Analysis

It is well known that Melnikov theory is one of the few analytical tools to study the global behaviour of a dynamical system. It helps to define the condition for the existence of the so-called transversal intersection of stable and unstable manifolds of homoclinic orbits. This may imply the occurrence of the so-called horseshoes structure of chaos.

Consider the generalized dynamical equation of a given system written in the vector form

$$\dot{q} = g_0(q) + \varepsilon g_p(q,t), \tag{4}$$

where $q = (x,y)$ with $y = \dot{x}$ is the state vector, $g_0 = (g_1, g_2)$ is the vector field according to the chosen Hamiltonian with the energy H_0 so that $g_1 = \frac{\partial H_0}{\partial y}$ and $g_2 = \frac{-\partial H_0}{\partial x}$, and g_p is a periodic perturbation function.

Let us assume that the unperturbed Hamiltonian system possesses a closed homoclinic orbit through the hyperbolic saddle point, because homoclinic orbits have been identified as a possible source of chaos. In the presence of the perturbation $g_p(q,t)$, the homoclinic orbit can be broken to yield the transverse intersection of stable and unstable manifolds, which gives rise to chaotic behaviour near the separatrix.

The Melnikov function measuring the distance between the stable and unstable manifolds in the Poincaré section for the perturbed system is defined by

$$M(t_0) = \int_{-\infty}^{+\infty} g_0(q^0(t)) \wedge g_p(q^0(t), t+t_0)\mathrm{d}t, \tag{5}$$

where "$\wedge$" denotes the exterior product of vectors, and $q^0(t)$ is the unperturbed homoclinic or hetoroclinic orbit written as $(x_0(t), y_0(t))$. If $M(t_0)$ has simple zeros with $M(\tau) = 0$ and $\frac{dM(t_0)}{dt_0} \neq 0$ at $t = \tau$ (conditions for transversal intersection), then a homoclinic or hetoroclinic bifurcation occurs, signifying the possibility of chaotic behaviour.

Here we rewrite (2) in form of a perturbation of a Hamiltonian system

$$\dot{x} = y,$$
$$\dot{y} = -\alpha x - \beta x^3 - \delta x^5 + \varepsilon[\mu(1-x^2)y + f\cos\omega t], \quad (6)$$

where ε is a small parameter $(0 < \varepsilon \ll 1)$ characterizing the smallness of the force and dissipative terms. The unperturbed system $(\varepsilon = 0)$ is a integrable Hamilton system with Hamiltonian

$$H(x,y) = \frac{1}{2}y^2 + \frac{\alpha}{2}x^2 + \frac{\beta}{4}x^4 + \frac{1}{6}\delta x^6. \quad (7)$$

We consider the case of a triple potential well, i. e. $\beta < 0$, α and $\delta \geq 0$. Through the analysis of the fixed points (x_i, y_i) and their stability one can see that five equilibrium points exist when $\Delta = \beta^2 - 4\alpha\delta > 0$: three stable center points at $(0,0)$ and $(\pm x_2, 0)$, and two unstable saddle points at $(\pm x_1, 0)$ where $x_1 = \sqrt{-\frac{1}{2\delta}(\beta + \sqrt{\Delta})}$ and $x_2 = \sqrt{-\frac{1}{2\delta}(\beta - \sqrt{\Delta})}$.

Thus there are two different types of orbits for each hyperbolic fixed point: a heteroclinic orbit connecting the two saddle points and a symmetric pair of homoclinic trajectories connecting each unstable saddle point to itself, which are given by

$$\begin{aligned} x_0(t) &= \pm\frac{\sqrt{2}x_1\cosh(\frac{\gamma}{2}t)}{\sqrt{\xi + \cosh(\gamma t)}}, \\ y_0(t) &= \pm\frac{\sqrt{2}\gamma(\xi-1)\sinh(\frac{\gamma}{2}t)}{2(\xi+\cosh(\gamma t))^{\frac{3}{2}}}, \end{aligned} \quad (8)$$

where $\gamma = x_1^2\sqrt{2\delta(\rho^2-1)}$, $\xi = \frac{5-3\rho^2}{3\rho^2-1}$ and $\rho^2 = \frac{\beta-\sqrt{\Delta}}{\beta+\sqrt{\Delta}}$.

Now let us turn our attention to the perturbed system $(\varepsilon \neq 0)$ and compute the Melnikov integrals (5). For this system, $g_0(q) = (y, -\alpha x - \beta x^3 - \delta x^5)$ and $g_p(q,t) = (0, \mu(1-x^2)y + f\cos\omega t)$. Then the Melnikov function $M(t_0)$ shown in (5) can be written as

$$M(t_0) = \int_{-\infty}^{+\infty} y_0[\mu(1-x_0^2)y_0 + f\cos\omega(t+t_0)]\,dt. \quad (9)$$

Substituting the expressions of the homoclinic trajectories (8) into (9) and calculating some integrals, we have

$$M_{\pm}(t_0) = D_0 \pm D_1\sin\omega t_0, \quad (10)$$

where

$$D_0 = \frac{\mu x_1^2\gamma}{4(1+\xi)}\left[\xi + 2 + \frac{x_1^2(\xi-1)}{(1+\xi)}\left(\xi^3 + \xi^2 + \frac{\xi-2}{3}\right) + \left(\frac{2\xi+1}{\sqrt{1-\xi^2}} + \frac{x_1^2\xi}{1+\xi}\right)\left(\arcsin\xi - \frac{\pi}{2}\right)\right]$$

and

$$D_1 = 2fx_1\sin\frac{2\omega}{\gamma}. \quad (11)$$

We are interested in such parameters f for which $M(t_0)$ has simple zeros for some value τ of t_0. $M(t_0)$ has a simple zero, if

$$|\frac{D_0}{D_1}| < 1. \quad (12)$$

Hence, a sufficient condition for the appearance of chaos in the sense of Smale is given by

$$f > -\frac{\mu x_1\gamma}{8(1+\xi)}\left[\xi + 2 + \frac{x_1^2(\xi-1)}{(1+\xi)}\left(\xi^3 + \xi^2 + \frac{\xi-2}{3}\right) + \left(\frac{2\xi+1}{\sqrt{1-\xi^2}} + \frac{x_1^2\xi}{1+\xi}\right)\left(\arcsin\xi - \frac{\pi}{2}\right)\right] \Big/ \sin\frac{2\omega}{\gamma}. \quad (13)$$

From this relation, the threshold values of the parameters for homoclinic chaos to occur can be obtained. The analytical prediction provided by (13) can be verified using a direct numerical simulation of the differential equation (2). It is found that the analytical treatment predicts in general too low a threshold for chaos. For instance, for a given set of parameters $\omega = 1.5$, $\mu = 0.3$, $\alpha = 0.385$, $\beta = -0.57$, $\delta = 0.16$ of the system (6), the critical value obtained from the direct analytical prediction (13) is $f \cong 0.24$ while the numerical simulation of (6) gives $f \cong 0.33$. This gap had also been observed in other physical models such as the ϕ^4 model, the magnetic pendulum and multiple equilibrium systems [12].

3. Numerical Simulation

In this section we use some effective numerical tools such as bifurcation diagrams, the largest Lyapunov exponent, the Poincaré map and phase plane plot, and the fractal dimension to study the dynamical behaviours and chaotic attractors of the system (2). Equation (2) can be equivalently written as

$$\begin{aligned} \dot{X} &= Y, \\ \dot{Y} &= f\cos\omega t + \mu(1-X^2)Y - \alpha X - \beta X^3 - \delta X^5. \end{aligned} \tag{14}$$

Equation (14) is numerically solved by applying the fourth-order Runge-Kutta (RK4) algorithm. Indeed, the RK4 algorithm is capable of much greater precision than Euler, and is probably the most popular. In the present study, we use the numerical ODE solvers: [rkf45] or [dverk78] in Maple, which is called the fourth-fifth order Runge-Kutta-Fehlberg method and seventh-eighth order Runge-Kutta-Fehlberg method. These methods are able to provide highly accurate solutions.

Let us study system (14) with a triple well potential. Choosing the system parameters $f = 1.80$, $\mu = 0.68$, $\alpha = 0.22$, $\beta = -0.58$, and $\delta = 0.16$, the dynamical responses of (14) by varying ω are described in Figure 2a. The corresponding largest Lyapunov exponents are computed in Fig. 2b, which confirm the existence of chaotic regions and periodic orbits. From Fig. 2a, we can see that the nonlinear dynamic system exhibits periodic and chaotic behaviours as the control parameter ω is changed. The smeared region in the bifurcation diagram indicates that the attractor of the system has a complex structure in parameter space, which manifests the complexity of the system's behaviour.

The onset of chaos occurs at $\omega = 1.141$, the corresponding largest Lyapunov exponent is 0.067. After the system has become chaotic, a number of windows of periodic behaviour appears. If the parameter ω increases to 1.292, the response of the system (14) goes back to a regular motion, and then through a narrow chaotic region in the interval $\omega \in (1.357, 1.410)$. After that a broad period-3 window is observed. As ω increases further, the system enters a next chaotic region from period-3 orbit via an intermittent or explosive bifurcation at $\omega = 1.917$, and finally returns to periodic motion by a cascade of inverse period-doubling bifurcations. Figure 3 displays the chaotic attractor in the phase portrait and Poincaré section at $\omega = 1.393$, and the corresponding largest Lyapunov exponent is 0.195.

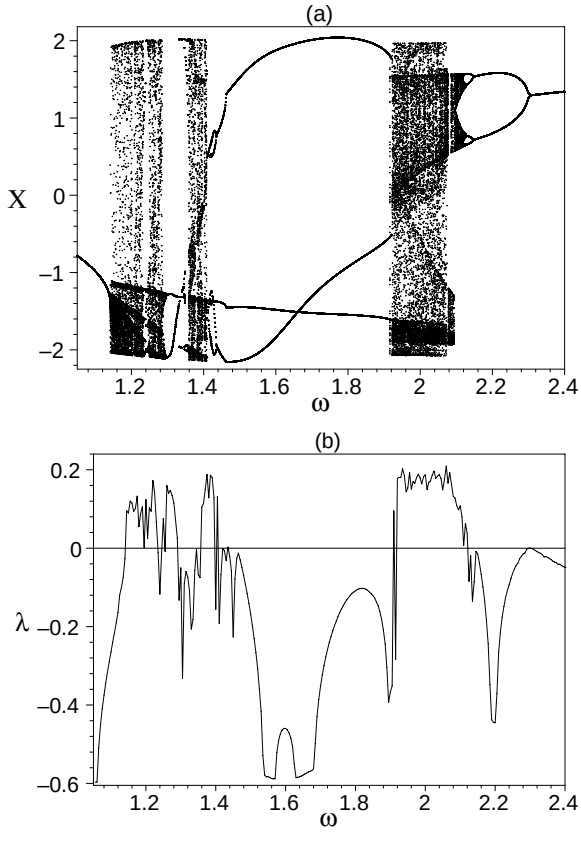

Fig. 2. (a) Bifurcation diagram in the (ω, X) plane of (14), with $f = 1.80$, $\mu = 0.68$, $\alpha = 0.22$, $\beta = -0.58$, and $\delta = 0.16$; (b) the largest Lyapunov exponent corresponding to (a).

From Fig. 2a we can also observe that there is an interior crisis where the chaotic attractor suddenly changes in size at $\omega = 2.075$. For clarity, Fig. 4 is used to demonstrate two different shapes of Poincaré sections of the strange attractors near the interior crisis. Figure 3a and b depict the phase trajectories and the Poincaré map of the chaotic attractor at $\omega = 2.074$, while the Poincaré map of the attractor at $\omega = 2.075$ is shown in Figure 4c. The largest Lyapunov exponents corresponding to the states in Figs. 4a,b and c are, respectively, 0.171 and 0.164.

In order to obtain better insight into the chaos features, we may calculate the fractal dimensions, called Lyapunov dimensions, of the strange attractors according to the definition of Kaplan and Yorke [13]

$$D_{\mathrm{L}} = k + \frac{1}{|\lambda_{k+1}|}\sum_{i=1}^{k}\lambda_i, \tag{15}$$

where k is defined by the condition that $\sum_{i=1}^{k}\lambda_i \geq 0$

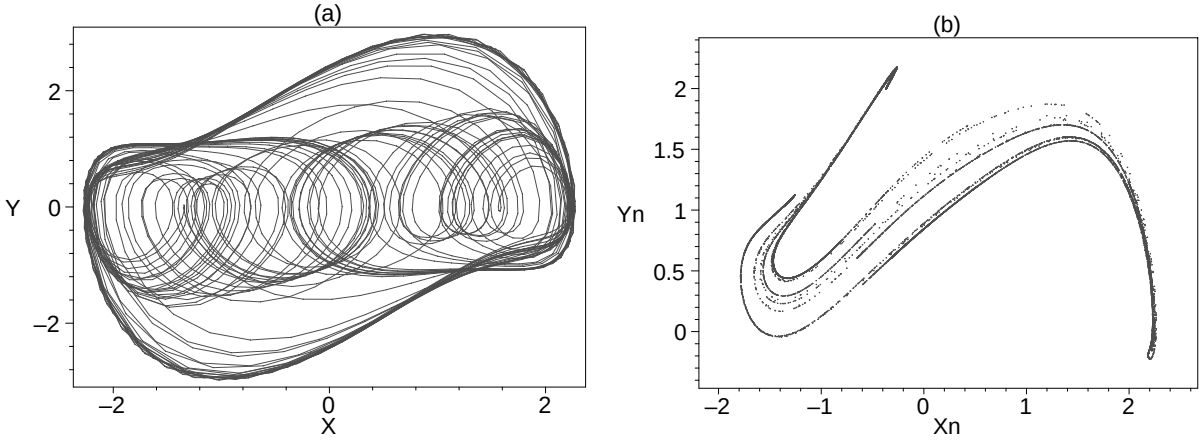

Fig. 3. (a) Phase projection of the chaotic state at $\omega = 1.393$ in Fig. 2a; (b) the Poincaré map corresponding to (a).

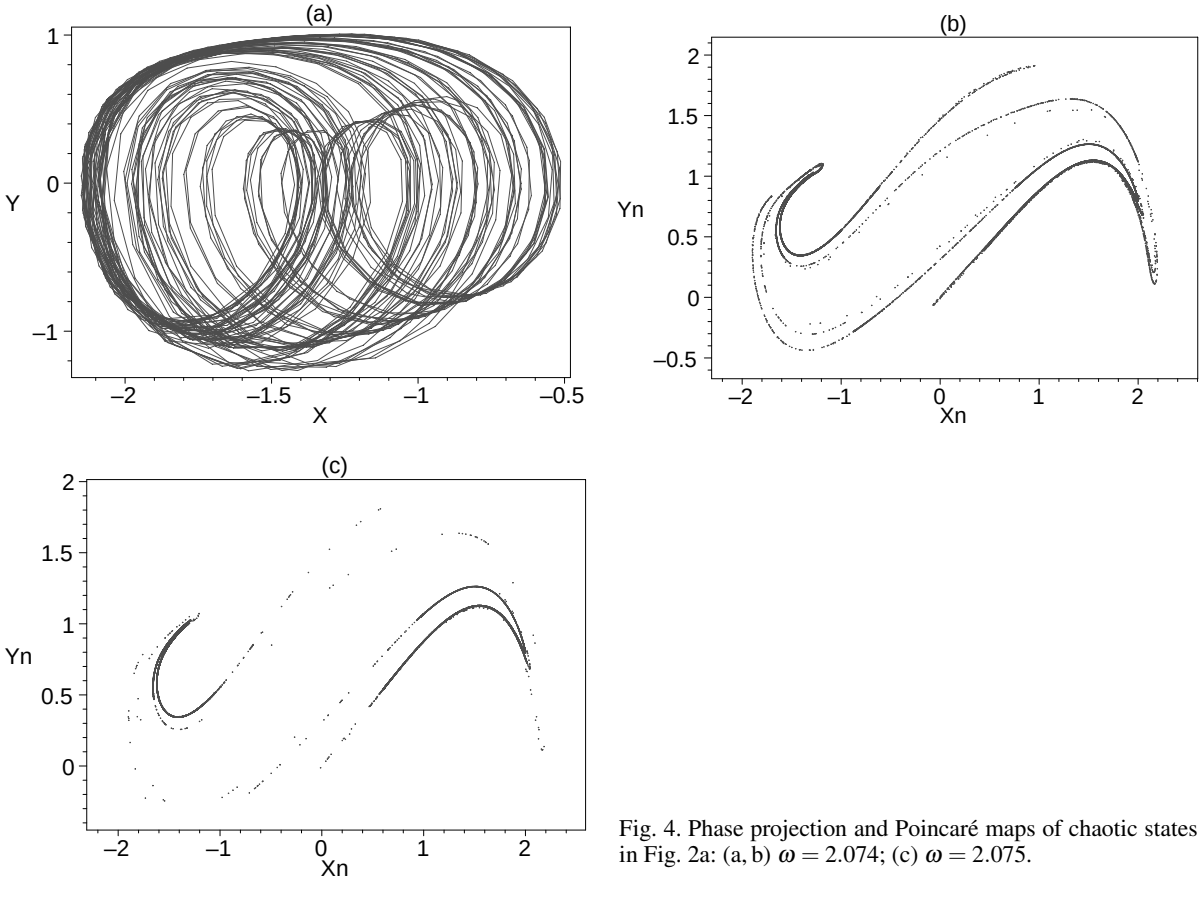

Fig. 4. Phase projection and Poincaré maps of chaotic states in Fig. 2a: (a, b) $\omega = 2.074$; (c) $\omega = 2.075$.

and $\sum_{i=1}^{k+1} \lambda_i < 0$. For example, the fractal dimension of the strange attractor ($\omega = 1.393$) shown in Fig. 3 is $D_{\mathrm{L}} = 2.227$. The fractal dimensions of the attractor given in Fig. 4b ($\omega = 2.074$) is $D_{\mathrm{L}} = 2.179$.

We now turn to consider system (14) in a single well case. Fixing $f = 3.25$, $\mu = 1.00$, $\alpha = 0.12$, $\beta = 0.78$ and $\delta = 0.50$, and change the parameter ω. The dynamical responses of system (14) with vary-

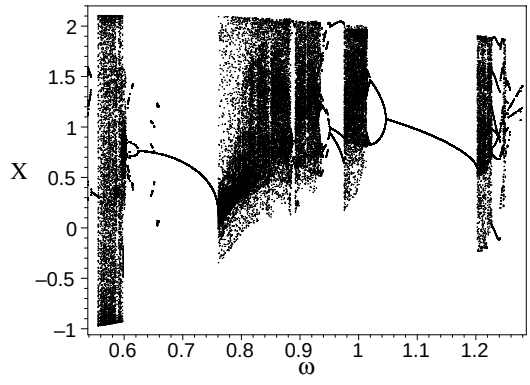

Fig. 5. Bifurcation diagram in the (ω, X)-plane of (14) with $f = 3.25$, $\mu = 1.00$, $\alpha = 0.12$, $\beta = 0.78$, and $\delta = 0.50$.

ing ω is described in Figure 5. Chaotic solutions and period-doubling cascades in the system are clearly visible.

4. Conclusion and Discussion

To sum up, we have studied the dynamics of the ϕ^6 Duffing-Van der Pol oscillator with a single well and triple well potentials. The criteria for the appearance of horseshoe chaos is derived by using the Melnikov theory. Make use of Maple software, we computed a great number of diagrams, and some of them showing the main features of the system are presented in Figures 2 – 5. It is shown that the dynamical chaos can occur if appropriate system parameters and initial conditions are chosen. It is worth mentioning that the bifurcation diagrams of system (14) containing a quintic nonlinear term are qualitatively different from that of Duffing-Van der Pol oscillator with a cubic nonlinear restoring force only (see [8]). Duing to the strong nonlinearity of the quintic term, this differences is not just a simple deformation or a shift. It can be observed from our obtained diagrams that the system goes to chaos from regular motions (or vice versa) usually through a sequence of period-doubling bifurcations, intermittencies and crisis. But in [8], the quasi-periodic route leading to chaos emerges frequently when the system parameters of the forced Duffing-Van der Pol oscillator are fixed to some special values [8]. Naturally, the dynamics exhibited by ϕ^6 Duffing-Van der Pol oscillator is also some distinct compared to the forced Duffing-Van der Pol oscillator.

Although the rich dynamics of the extended Duffing-Van der Pol oscillator (2) has been explored by theoretic analysis and numerical simulations, it should be pointed out that there are abundant and complex dynamical behaviours still unknown in this new system, which may contribute to the better understanding of the essence. From this point of view, it is believed that the new oscillator deserves further investigation in the near future.

Acknowledgement

The work was supported by the National Natural Science Foundation of China (Grant No. 10875078) and the Natural Science Foundation of Zhejiang Province of China (Grant No. Y7080455). The authors are grateful to Prof. Lutz Schimansky-Geier and Dr. Tiak Wan Ng for their valuable discussions. We also would like to express our sincere thanks to the referees for their useful suggestions.

[1] M. Lakshmanan and K. Murali, Chaos in Nonlinear Oscillators: Controlling and Synchronization, World Scientific, Singapore 1996.
[2] A. N. Njah and U. E. Vincent, Chaos, Solitons and Fractals **37**, 1356 (2008).
[3] J. Yu, W. J. Zhang, and X. M. Gao, Chaos, Solitons and Fractals **33**, 1307 (2007).
[4] J. Guckenheimer and P. Holmes, Nonlinear Oscillation and Bifurcation of Vector Filds, Springer, New York 1993.
[5] B. J. A. Zielinska, D. Mukamel, V. Steinberg, and S. Fishman, Phys. Rev. **A32**, 702 (1985).
[6] F. M. Moukam Kakmeni, S. Bowong, C. Tchawoua, and E. Kaptouom, J. Sound Vib. **277**, 783 (2004).
[7] Y. Ueda and N. Akamatsu, IEEE Trans. Circuits Systems CAS-**28**, 217 (1981).
[8] A. Venkatesan and M. Lakshmanan, Phys. Rev. **E56**, 6321 (1997).
[9] M. Siewe Siewe, F. M. Moukam Kakmeni, and C. Tchawoua, Chaos, Solitons and Fractals **21**, 841 (2004).
[10] X. L. Yang, W. Xu, and Z. K. Sun, Chaos, Solitons and Fractals **27**, 778 (2006).
[11] F. M. Moukam Kakmeni, S. Bowong, C. Tchawoua, and E. Kaptouom, Phys. Lett. **A322**, 305 (2004).
[12] F. C. Moon, Chaos and Fractal Dynamics, Wiley, New York 1992.
[13] H. Kaplan and J. A. Yorke, Lecture Note in Mathematics, Springer-Verlag, Berlin 1979.